Volume 20 | Number 35 | 21 September 2018 | Pages 5081–5282

CrystEngComm

rsc.li/crystengcomm

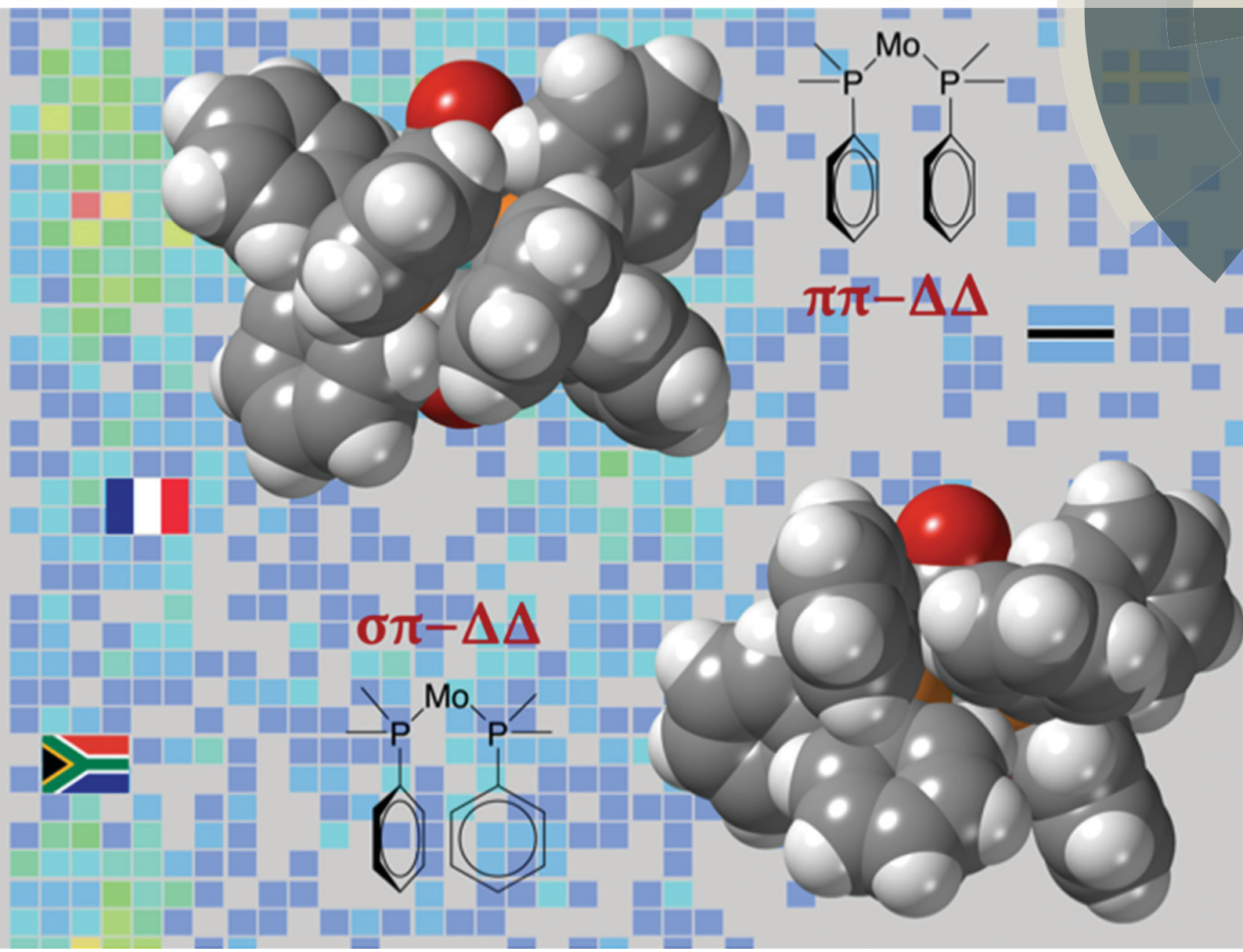

ROYAL SOCIETY OF CHEMISTRY

PAPER

Never Tshabang, Susan A. Bourne, François-Xavier Coudert, Lars Öhrström *et al.*

Conformational chiral polymorphism in *cis*-bis-triphenylphosphine complexes of transition metals

CrystEngComm

PAPER

View Article Online
View Journal | View Issue

Cite this: *CrystEngComm*, 2018, **20**, 5137

Conformational chiral polymorphism in *cis*-bis-triphenylphosphine complexes of transition metals†

Never Tshabang,*[a] Gaone P. Makgatle,[a] Susan A. Bourne,*[b] Nina Kann,[c] Jack D. Evans,‡[d] François-Xavier Coudert*[d] and Lars Öhrström*[c]

The structure of *cis*-[Mo(CO)$_4$(PPh$_3$)$_2$] **1** was determined by F. A. Cotton, D. J. Darensbourg, S. Klein and B. W. S. Kolthammer, *Inorg. Chem.*, 1982, **21**, 1651–1655, with the space group $P\bar{1}$. A second polymorph **2** is reported here, with the space group $P2_1/c$. The compounds differ in the interactions between the conformational chiral triphenylphosphine groups. In **1**, there is π–π stacking between adjacent phenyl groups, whereas in **2**, there are σ–π interactions instead. A search of the Cambridge Structural Database reveals that this is a relatively frequent occurrence in *cis*-bis-triphenylphosphine complexes and the phenomenon can be analysed by means of the C(ipso)–P–M–P torsion angles. The majority of compounds fall in the π–π stacking data area with torsion angles of 10–15° and 55–60°; however, for octahedrally coordinated metals, the optimum is a σ–π interaction at 40°/40°. This corresponds well to the values in **2**: 46°/40°, but for **1**, we instead find the torsion angles to be 11°/18°. There is indeed a small occurrence of these values as well in the data, and it appears that for **1**, this conformation is stabilised by weak CO···H–C hydrogen bonds. Density functional theory (DFT) calculations indicate that **1** is the more stable polymorph by 72 kJ mol^{-1} but that the strain of the complexes (the difference between a relaxed molecule in the respective conformation and the structure in the crystal) is larger for **1** than for **2**, further indicating that a special intermolecular interaction is responsible for the stability of this polymorph. In both polymorphs, the triphenylphosphines have the same conformational chirality, consistent with single-molecule calculations that predict racemic conformations to be substantially higher in energy for both σ–π interactions (+17 kJ mol^{-1}) and π–π stacking (+30 kJ mol^{-1}).

Received 2nd March 2018,
Accepted 1st June 2018

DOI: 10.1039/c8ce00337h

rsc.li/crystengcomm

1. Introduction

Triarylphosphines are ubiquitous in organometallic chemistry. As early as 1948, Reppe used [NiBr$_2$(PPh$_3$)$_2$],[2] and ever since the preparation of Wilkinson's catalyst, [RhCl(PPh$_3$)$_3$], in 1965 (ref. 3) and the subsequent employment of triphenylphosphine and its derivatives as ligands to transition metal catalysts in industrial processes, for example hydroformylation,[4] they have been trustworthy work horses for the organometallic and catalysis community.[5]

PPh$_3$ continues to play an important role in catalysis to this day; examples include the use of [Pd(PPh$_3$)$_4$] in classical cross-coupling reactions with aryl halides,[6] applications of diphosphine complexes such as [PdCl$_2$(PPh$_3$)$_2$] in carbonylative Sonogashira reactions,[7,8] and as a [RuCl(phenpy-OH)(PPh$_3$)$_2$]PF$_6$ catalyst in the β-alkylation of secondary alcohols with primary alcohols.[9] Looking at other metal-PPh$_3$ complexes, iron catalysts such as [Fe(H)(CO)(NO)(PPh$_3$)$_2$] and [Fe(CO)Cp(PPh$_3$)I] have been applied in the hydrosilylation of alkynes[10] and acetophenone,[11] respectively, while cobalt complexes like [Co(H)(N$_2$)(PPh$_3$)$_3$] or [CoH$_3$(PPh$_3$)$_3$] can effect CH-activation of aromatic compounds.[12] A recent application of interest involves the dual use of [Ph$_3$PAuCl] and visible light to achieve the synthesis of biarylic compounds *via* a Suzuki-type coupling.[13] Triphenylphosphine has also been employed in itself as an

[a] *Department of Chemistry, Faculty of Science, University of Botswana, Gaborone, Botswana. E-mail: tshabang@mopipi.ub.bw*
[b] *Centre for Supramolecular Chemistry Research, Department of Chemistry, University of Cape Town, Rondebosch 7701, Cape Town, South Africa. E-mail: susan.bourne@uct.ac.za*
[c] *Chemistry and Biochemistry, Dept. of Chemistry and Chemical Engineering, Chalmers University of Technology, SE-41296 Göteborg, Sweden. E-mail: ohrstrom@chalmers.se*
[d] *Chimie ParisTech, PSL University, CNRS, Institut de Recherche de Chimie Paris, 75005 Paris, France. E-mail: fx.coudert@chimieparistech.psl.eu*

† Electronic supplementary information (ESI) available: Figure S1. CCDC 1499384 contains the supplementary crystallographic data for compound 2. For ESI and crystallographic data in CIF or other electronic format see DOI: 10.1039/c8ce00337h

‡ Current address: Anorganische Chemie I, Fachrichtung Chemie und Lebensmittelchemie, Technische Universität Dresden, Bergstraße 66, 01062 Dresden, Germany.

organocatalyst in reactions of allenes with electrophiles,[14] as well as in [2 + 2 + 2]-annulations to form dihydropyridine structures.[15]

That triarylphosphines are conformationally chiral was realised long ago,[16,17] and they have been subjected to detailed studies,[18] but such analyses of bis-triphenylphosphine complexes are scarce. In this communication, we report on a new polymorph of *cis*-[Mo(CO)$_4$(PPh$_3$)$_2$] **2** in the space group $P2_1/c$, distinct from the earlier reported $P\bar{1}$ polymorph **1** in terms of both phosphine configurations and intermolecular interactions. We have also placed this finding in a broader context by analysing diphosphine complexes in the Cambridge Structural Database (CSD) and performing quantum chemical calculations on both crystals and single molecules.

In principle, one could envisage four different ways in which these molecules could vary in their conformations. We could think of either σ–π interactions or π–π stacking as potentially being the most favoured intramolecular interaction between the closest phenyl groups of the two triphenylphosphine units. Added to this is the possibility of having either homo (ΔΔ or ΛΛ) or heterochiral triphenylphosphines, giving a total of four possible conformers: σπ–ΔΔ, σπ–ΔΛ, ππ–ΔΔ, and ππ–ΔΛ. Considering also the possibility of different packings, the potential for polymorphism seems rather large. However, it is quite possible that some of the conformers have too high energies to be accessible, even if a favoured packing can be arranged.

2. Experimental

2.1 Materials and methods

2.1.1 X-ray crystallography. Intensity data were collected using a Bruker Apex II diffractometer with Mo Kα radiation (λ = 0.7107 Å). Unit cell determinations were carried out both at ambient temperature (294 ± 2 K) and at low temperature (173 ± 2 K) in order to test whether there were any phase changes during the cooling process; none were evident. The structure of **2** was solved routinely using SHELXS-64 and refined against F^2 with SHELXL-64.[19]

The structure determination details are found in Table 1, and an ORTEP type drawing for the molecular unit is shown in Fig. 1.

2.1.2 Searching the Cambridge Crystallographic Database. The CSD database 5.38 (February 2017) was used. In all runs, the Conquest software (version 1.19) was used with the restrictions that all retrieved structures would have R values <10% and be error- and disorder-free. No powder structures were included.

2.1.3 Computational details. Density functional theory (DFT) simulations were applied using the Crystal14 software developed by Dovesi and coworkers.[20] We used the PBESOL0 functional[21] in conjunction with the POB triple-zeta valence + polarization basis set for C, O, P, and H elements,[22] and Mo was treated with a small-core effective-core pseudopotential of the Hay-Wadt type described by Corà *et al.*[23] The geometries of the single molecules and crystal structures were optimized using default convergence criteria. Optimizations of the crystal structures included relaxing both the atomic coordinates and the parameters of the cell. Lattice energy is defined as the difference in energy between the crystal and the free molecule in its relaxed form. Packing energy is calculated as the difference in energy between the crystal and the individual molecule in the same conformation as in the

Table 1 Crystallographic parameters for **1** (Cotton, ref. 1) and **2** (this work)

	1[a]	**2**
Empirical formula	$C_{40}H_{30}MoO_4P_2$	$C_{40}H_{30}MoO_4P_2$
Molecular mass (g mol^{-1})	732.52	732.52
Crystal size (mm)		0.03 × 0.09 × 0.16
Temperature of data collection	298	173(2)
Crystal symmetry	Triclinic	Monoclinic
Space group	$P\bar{1}$	$P2_1/c$
a (Å)	11.522(1)	9.4289(7)
b (Å)	16.909(3)	38.395(3)
c (Å)	9.633(2)	9.9447(7)
α (°)	98.05(2)	90
β (°)	110.29(1)	107.876(1)
γ (°)	99.95(1)	90
Z	2	4
Volume (Å^3)	1692.73(4)	3426.4(4)
Density$_{calc}$ (g cm^{-3})	1.437	1.420
2θ range scanned (°)		2.12–27.95
F (000)		1496
No. of reflections collected		57 328
No. of unique reflections		8215
No. of reflections with $I > 2\theta$		6229
Goodness of fit, S		1.016
R_1 ($I > 2\sigma I$)	0.043	0.0392
Final wR_2 (all data)		0.0857
Min, max e density/e		−0.470, 0.540

[a] Cotton *et al.*[1]

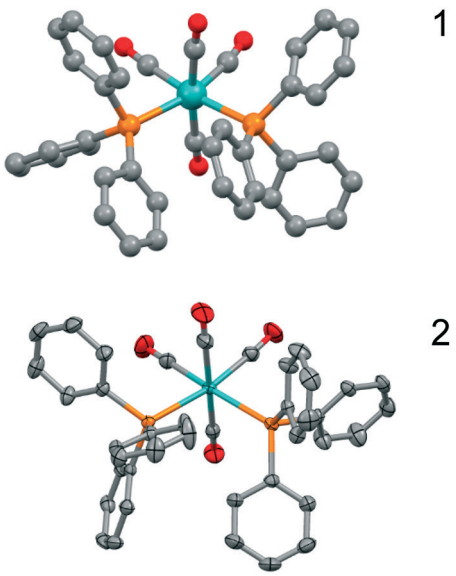

Fig. 1 Drawings of the molecular units of **1** (top, ball-and-stick) and **2** (bottom, ORTEP type). Hydrogen atoms are omitted for clarity.

crystal. The difference between the lattice energy and packing energy is defined as the strain energy which is attributed to the deformation of the molecule within the lattice. The geometries of the single molecules and crystal structures were optimized using default convergence criteria and the shrink parameter was set to 2. Input files for the calculations and optimized structures can be found online at https://github.com/fxcoudert/citable-data.

2.2 Synthesis

2.2.1 Synthesis of 2, *cis*-[Mo(CO)$_4$(PPh$_3$)$_2$] in the space group $P2_1/c$. To a 250 mL two-neck round-bottomed flask equipped with a stirrer bar, [Mo(CO)$_3$(1,3,5-trimethylbenzene)] (0.2919 g, 0.9773 mmol) and PPh$_3$ (0.8813 g, 3.364 mmol) were added under a nitrogen atmosphere. THF (in 50 mL) was then added, and the solution was kept under reflux for 1 hour. The reaction mixture turned from the initial colour of yellow to dark orange. The product was obtained as light yellow crystals after reducing the volume of the solution to ~10 mL, and then adding 20 mL of petroleum ether (60–80 °C) and collecting the crystals of 2 by suction filtration. Yield: 58%. FT-IR (Nujol, cm^{-1}): ν(C≡O) 2013, 1899, and 1877. ^{1}H NMR (CD_2Cl_2, 300.13 MHz) δ: 7.26–7.41 (m, 30 H, Ph) ppm. ^{31}P NMR (CD_2Cl_2, 75.47 MHz); δ = 37.7 ppm. Single crystals of the compound, suitable for X-ray crystallographic analysis, were obtained by slow diffusion of hexane into a solution of 2 in dichloromethane for a period of one week. The crystals were sent to the University of Cape Town for X-ray crystallographic analysis.

3. Results and discussion

3.1 Synthesis

Crystals of *cis*-[Mo(CO)$_4$(PPh$_3$)$_2$] in the space group $P2_1/c$ 2 were obtained when the synthesis of *fac*-[Mo(CO)$_3$(PPh$_3$)$_3$] was attempted by the method for preparing *fac*-[Cr(CO)$_3$(PPh$_3$)$_3$] reported by Nicholls and Whiting.[24] Crystals suitable for single crystal X-ray diffraction were obtained by slow diffusion of hexane into a solution of 2 in dichloromethane for a period of one week. It should be noted that the previously reported crystals 1 of *cis*-[Mo(CO)$_4$(PPh$_3$)$_2$] in the space group $P\bar{1}$ were obtained by recrystallizations from a chloroform/methanol mixture at 0 °C.[1] This underpins the important role of the solvent during crystallisation.

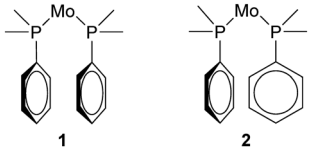

1 2

Fig. 2 Schematic difference between the bis-phosphine units in 1 and 2.

3.2 X-ray crystallography structure analysis

The structure determination details are displayed in Table 1 and an ORTEP type drawing for the molecular unit is shown in Fig. 1.

On the bonding level, 1 and 2 are very similar as the Mo–C and Mo–P bonds are close (Mo–P, 2.58 Å *vs.* 2.58 Å, Mo–C, 1.98–2.04 Å *vs.* 1.97–2.06 Å), but the configurations of the closest phenyl contacts between triphenylphosphine ligands are distinctively different, as shown schematically in Fig. 2, corresponding to the π–π- and σ–π-cases.

However, this is not a question of the two polymorphs having, in one case, the same configurational chirality on the phosphine ligands and the other one having opposite chiralities. In both cases, as far as can be quantified, the chirality is the same for the two phosphine ligands, but in neither case, the propeller-like chirality is perfect. Thus, what we have are the σπ–ΔΔ and ππ–ΔΔ conformers. In fact, judging from the physical ball-and-spoke molecular models, it seems difficult to have different chiralities on the two PPh$_3$ ligands and turn these into a sensible conformation that does not generate very close contacts. This, however, needs to be quantified and confirmed by quantum chemical calculations.

3.3 Structure calculations

To gain some insight into the factors playing a role in this polymorphism case, DFT calculations were performed, both under periodic boundary conditions on the two crystal systems, single molecule calculations for the chiral conformers 1 and 2, and the corresponding hypothetical non-chiral conformers 3 and 4.

The results in terms of energy are summarised in Table 2. First, we note that the small difference on a single molecule level for 1 and 2 is just about significant, as the two configurations will differ only because of relatively weak interactions between the phenyl rings. Second, on a structural level, the

Table 2 Energy calculations on the two polymorphs 1 and 2 and the hypothetical single-molecule non-chiral conformers σπ–ΔΛ 3 and ππ–ΔΛ 4

	Space group	Conformation	Relative crystal energy (kJ mol^{-1})	Lattice energy[a] (kJ mol^{-1})	Packing energy[b] (kJ mol^{-1})	Molecular strain in crystal[c] (kJ mol^{-1})	Single molecule energy difference (kJ mol^{-1})
1	$P\bar{1}$	ππ–ΔΔ	0	−245.6	−282.9	37.3	0
2	$P2_1/c$	σπ–ΔΔ	72.4	−235.6	−260.6	25.0	7.7
3	n.a.	σπ–ΔΛ					16.7
4	n.a.	ππ–ΔΛ					30.3

[a] Lattice energy is the difference in energy between the crystal and the free molecule in its relaxed form. [b] Packing energy is the difference in energy between the crystal and the individual molecule in the same conformation as in the crystal. [c] Lattice energy = packing energy + strain energy from the deformation of the molecule to fit into the crystal lattice.

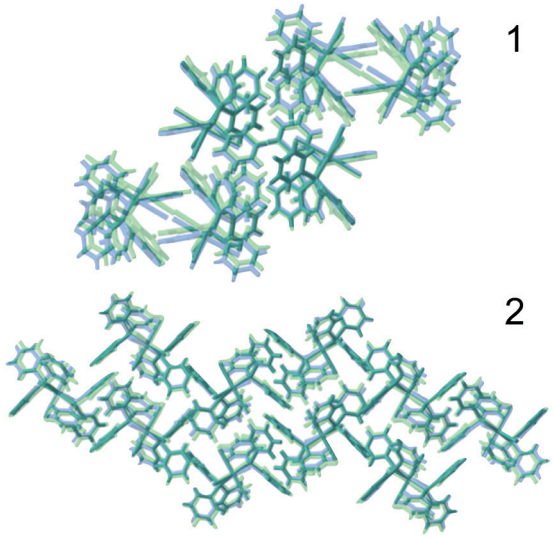

Fig. 3 Comparison of experimental (blue) and optimised structures (green) of **1** (top) and **2** (bottom).

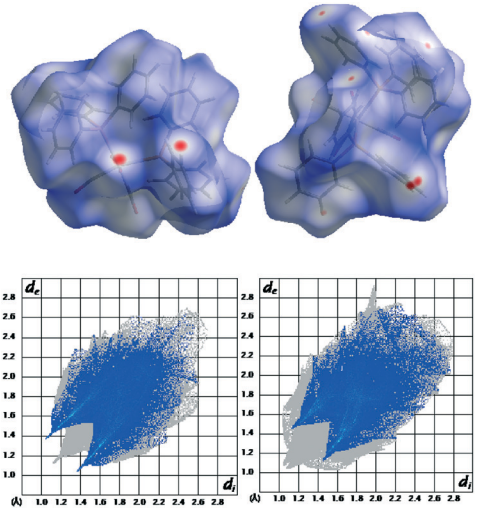

Fig. 5 Top: Hirshfeld surface analysis of **1** (left) and **2** (right), bottom: Hirshfeld surface analysis fingerprint plots of **1** (left) and **2** (right); O···H interactions are emphasised. The perspectives are different to show the major interactions for both compounds.

two polymorphs are well reproduced by the calculations (see Fig. 3).

The four molecular conformers **1**–**4** are displayed in Fig. 4.

On a crystal level, **1** is the more stable polymorph, consistent with its higher density (Table 1). There may also be more specific interactions that evoke a more stable polymorph. Hirschfeld surface analysis[25–27] (Fig. 5) indicates one fairly strong double CO···H interaction at 2.135 Å, O···C at 3.190 Å, and CHO at 163.8° (calc.) and 2.5404 Å, 3.490 Å, and 177.7° (exp.). These are short, and C···O (the best determined distance) is very close to the optimum C–H···OC distance which is 3.48 Å according to analysis of data in the CSD. However, the optimum angle is 116°, which is very far from the observed 177.7° (see the ESI,† Fig. S1).

The fingerprint plot also reveals a higher H···H repulsion in **2** (the peaks pointing to the lower left along the diagonal). However, the strain induced in the two conformers going from the free single molecules to the crystal is larger by 12.3 kJ mol^{-1} for **1**. This can also be quantified on a structural level as the total difference between the C_{ipso}–P–Mo–P torsion angles between the optimised free molecule and the molecule restricted in the crystal is almost double for **1** compared to **2** (see Table 3).

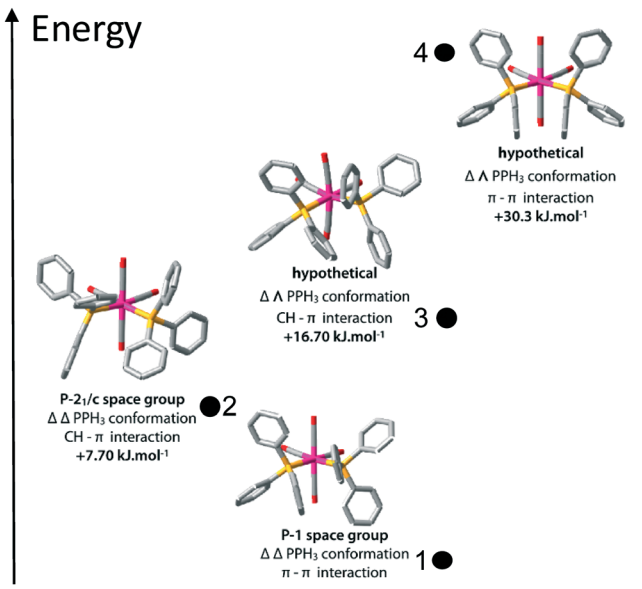

Fig. 4 Optimized structures of the four conformations of *cis*-$[Mo(CO)_4(PPh_3)_2]$. The two lowest energy conformers correspond to the experimentally observed compounds **1** and **2**.

3.4 Cambridge Structural Database analysis

These two C_{ipso}–P–M–P torsion angles (φ-angles) are also what we consider to be the best descriptors for the different conformations of the *cis*-$M(PPh_3)_2$-fragment when we searched the CSD to see which of these two conformations was the most common, or if there were indeed other conformations to consider as well. Torsion angles were selected for all *cis*-bis-triphenylphosphine fragments (P–M–P angles 90–105°), first for all the compounds, giving 1428 structures, and then with the restriction that the metal should be 6-coordinated just as the title compound, leaving us with 287 hits. The data are displayed in Fig. 6.

What emerges from this is that for lower coordination numbers, as for cyclopentadienyl complexes for example, there is more space for the PPh_3 to spread around the metal ion and this seems to generate a clear preference for a 15°/60° conformation. With the more crowded octahedral complexes, like **1** and **2**, the most common is instead the 40°/40° conformation. For six-coordinated compounds, there is also a weak tendency towards 20°/20°. This, however, does not tell

Table 3 Geometric data for the optimised structures of **1** and **2**

Comp.	Space gr.	In crystal φ_1 (°)	In crystal φ_2 (°)	Free molecule φ_1 (°)	Free molecule φ_2 (°)	Total abs. diff. free crystal	Ph⋯Ph in crystal β (°)	Ph⋯Ph free molecule β (°)
1	$P\bar{1}$	11.1	17.8	n.a.	n.a.		17.0	n.a.
1	$P\bar{1}$ DFT	10.0	17.1	20.1	20.6	13.6	20.7	6.3
2	$P21/c$	40.0	46.5	n.a.	n.a.		70.9	n.a.
2	$P21/c$ DFT	37.6	45.2	39.0	39.6	7.0	63.9	39.0

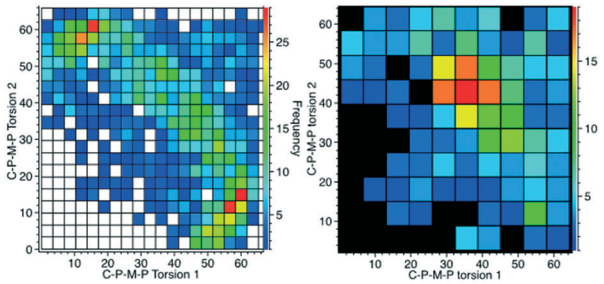

Fig. 6 CSD analysis of the C_{ipso}–P–M–P torsion angles for the *cis*-$M(PPh_3)_2$-fragment. Left: all data; right: with the restriction that M should be hexa-coordinated.

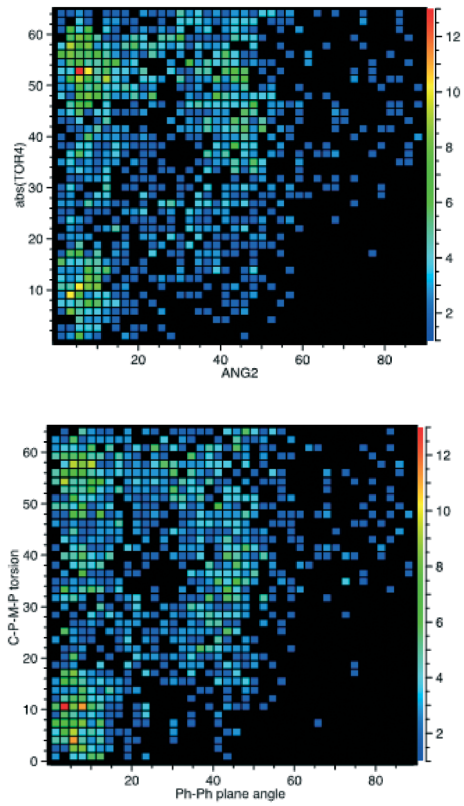

Fig. 7 CSD analysis of the C_{ipso}–P–M–P torsion angles for the *cis*-$M(PPh_3)_2$-fragment compared to the angle between the closest phenyl rings of the different PPh_3 ligands.

us anything about the closest phenyl rings exhibiting π-stacking or σ–π-interaction (Fig. 2).

Therefore, we also searched for pairwise C–P–M–P torsion angles less than 65°, as these will correspond to the closest phenyls, and then calculated the angles between the corresponding phenyl planes (β angles). For every angle between planes, there will thus be two torsion angles so two plots are needed to display these data, as shown in Fig. 7. These data show planar π-stacking for the 15°/60° conformation and σ–π-interaction for the 40°/40° conformation. This also corresponds well to the data for both **1** and **2**, as can be seen from the β angles also tabulated in Table 3.

We note that the quantum chemical calculations indicate that the homochiral conformation is preferred. This means that it could be possible to crystallise conglomerates where individual crystals are enantiomerically pure, either ΔΔ or ΛΛ. If this would be the case, these compounds should crystallise in any of the Sohncke space groups (chiral space groups that are without a centre of inversion). However, the most prominent space groups, accounting for 91% of the structures, are the non-Sohncke groups $P\bar{1}$ (#2) and $P2_1/c$ (#14), and the most occurring "chiral" space group, $P2_12_12_1$, is found only in 8 (3%) of the 287 structures.

That both the computational energy minima and distinct peaks in the CSD searcher are found means that the compounds fulfil the criteria for conformational polymorphism, as discussed by Cruz-Cabeza and Bernstein.[28]

4. Conclusions

Analysis of the CSD data indicates a multitude of possible bis-triphenylphosphine configurations and confirms the notion that both σ–π interactions and π–π stacking are possible.

However, quantum chemical calculations show that the heterochiral conformers are substantially higher in energy than the homochiral analogues.

Calculations on the entire crystal indicate, as expected, that the high density phase, **1**, is indeed lower in energy than **2**, which has a slightly lower density. Hirshfeld surface analysis indicates that a fairly strong double CO⋯H interaction may be one factor giving **1** the lower energy despite the fact that the conformation of the *cis*-$[Mo(CO)_4(PPh_3)_2]$ molecule in this structure is 12.3 kJ mol^{-1} more strained than in **2**.

Conflicts of interest

There are no conflicts to declare.

Acknowledgements

NT, GPM, NK and LÖ thank the Swedish Research Council for a Swedish Research Links grant. SB thanks UCT for the ICRP award. LÖ thanks Ambassade de France and Institut français in Stockholm for a travel grant. We acknowledge access to HPC platforms provided by a GENCI grant (A0030807069).

Notes and references

1 F. A. Cotton, D. J. Darensbourg, S. Klein and B. W. S. Kolthammer, *Inorg. Chem.*, 1982, **21**, 1651–1655.
2 W. Reppe and W. J. Schweckendiek, *Comp. Rendus*, 1948, **560**, 104–116.
3 J. A. Osborn, F. H. Jardine, J. F. Young and G. Wilkinson, *J. Chem. Soc. A*, 1966, 1711–1732.
4 R. Franke, D. Selent and A. Borner, *Chem. Rev.*, 2012, **112**, 5675–5732.
5 *Phosphorus(III) Ligands in Homogeneous Catalysis*, ed. P. C. J. Kamer and P. W. N. M. van Leeuwen, John Wiley & Sons, Ltd., Chichester, U. K., 2012.
6 A. F. Littke and G. C. Fu, *Angew. Chem., Int. Ed.*, 2002, **41**, 4176–4211.
7 H. Zhao, M. Z. Cheng, J. T. Zhang and M. Z. Cai, *Green Chem.*, 2014, **16**, 2515–2522.
8 L. A. Aronica, G. Albano, L. Giannotti and E. Meucci, *Eur. J. Org. Chem.*, 2017, 955–963, DOI: 10.1002/ejoc.201601392.
9 K. Chakrabarti, B. Paul, M. Maji, B. C. Roy, S. Shee and S. Kundu, *Org. Biomol. Chem.*, 2016, **14**, 10988–10997.
10 C. Belger and B. Plietker, *Chem. Commun.*, 2012, **48**, 5419–5421.
11 J. X. Zheng, L. C. M. Castro, T. Roisnel, C. Darcel and J. B. Sortais, *Inorg. Chem. Acta*, 2012, **380**, 301–307.
12 G. Halbritter, F. Knoch, A. Wolski and H. Kisch, *Angew. Chem., Int. Ed. Engl.*, 1994, **33**, 1603–1605.
13 C. Sauer, Y. Liu, A. De Nisi, S. Protti, M. Fagnoni and M. Bandini, *ChemCatChem*, 2017, **9**, 4456–4459.
14 Z. M. Wang, X. Z. Xu and O. Kwon, *Chem. Soc. Rev.*, 2014, **43**, 2927–2940.
15 H. M. Liu, Q. M. Zhang, L. M. Wang and X. F. Tong, *Chem. Commun.*, 2010, **46**, 312–314.
16 J. M. Brown and K. Mertis, *J. Organomet. Chem.*, 1973, **47**, C5–C7.
17 V. G. Albano, P. Bellon and M. Sansoni, *J. Chem. Soc. A*, 1971, 2420–2425, DOI: 10.1039/j19710002420.
18 J. F. Costello, S. G. Davies, E. T. F. Gould and J. E. Thomson, *Dalton Trans.*, 2015, **44**, 5451–5466.
19 G. M. Sheldrick, *Acta Crystallogr., Sect. C: Struct. Chem.*, 2015, **71**, 3–8.
20 R. Dovesi, R. Orlando, A. Erba, C. M. Zicovich-Wilson, B. Civalleri, S. Casassa, L. Maschio, M. Ferrabone, M. De La Pierre, P. D'Arco, Y. Noël, M. Causà, M. Rérat and B. Kirtman, *Int. J. Quantum Chem.*, 2014, **114**, 1287–1317.
21 J. P. Perdew, A. Ruzsinszky, G. I. Csonka, O. A. Vydrov, G. E. Scuseria, L. A. Constantin, X. Zhou and K. Burke, *Phys. Rev. Lett.*, 2008, **100**, 136406.
22 M. F. Peintinger, D. V. Oliveira and T. Bredow, *J. Comput. Chem.*, 2013, **34**, 451–459.
23 F. Cora, A. Patel, N. M. Harrison, C. Roetti, C. Richard and A. Catlow, *J. Mater. Chem.*, 1997, **7**, 959–967.
24 B. Nicholls and M. C. Whiting, *J. Chem. Soc.*, 1959, 551–556.
25 S. K. Wolff, D. J. Grimwood, J. J. McKinnon, D. Jayatilaka and M. A. Spackman, *CrystalExplorer*, University of Western Australia, Perth, Australia, 2007, http://crystalexplorer.scb.uwa.edu.au.
26 M. A. Spackman and J. J. McKinnon, *CrystEngComm*, 2002, **4**, 378–392.
27 J. J. McKinnon, M. A. Spackman and A. S. Mitchell, *Acta Crystallogr., Sect. B: Struct. Sci.*, 2004, **60**, 627–668.
28 A. J. Cruz-Cabeza and J. Bernstein, *Chem. Rev.*, 2014, **114**, 2170–2191.

